A New Femtosecond Laser-Based Tomography Technique for Multiphase Materials

McLean P. Echlin, Naji S. Husseini, John A. Nees, and Tresa M. Pollock*

Three-dimensional (3D) information on the distribution of elements or phases within inorganic and organic materials is often essential when material features are anisotropic or heterogeneously distributed. Such information is critical for developing predictive models for material properties and for optimizing processes for materials synthesis. We have developed a new tomography technique using the unique characteristics of femtosecond laser ablation for rapid serial sectioning and assembly of mm^3-scale 3D datasets. A protocol for controlled, cumulative deposition of millions of low-damage femtosecond laser pulses on the sample surface permits rapid layer-by-layer material ablation at precisely controllable rates. This fully automated technique provides new capabilities for imaging of multiphase materials with sectioning rates orders of magnitude faster than current mechanical or focused ion beam type techniques. An example is presented where 3D information on the mm-scale is captured for widely-dispersed nm-scale TiN particles in a steel alloy. We also demonstrate that chemical and microstructural information can be gathered simultaneously by incorporating laser-induced breakdown spectroscopy.

Tomographic imaging has provided major scientific insights to problems in medicine, geology, oceanography, astronomy and materials science.[1–5] Two-dimensional (2D) slices that can be reconstructed into 3D datasets are acquired with a wide variety of techniques that utilize electrons,[6] neutrons,[7] X-rays,[8] ions,[3,9] visible light[1,2] or acoustic waves.[10] The sectioning and imaging approach is constrained by the level of resolution required, physical size of the object being interrogated, nature of the interaction of the material(s) being imaged with the imaging probes, and destructive or non-destructive effects of the specific machining method. The availability of 3D information permits analysis of material features such as particle clustering,[11,12] spatial orientation and geometry,[13] and phase interconnectivity,[3] which are often misrepresented by 2D analysis of anisotropic materials.[14] For many materials, the rarely occurring features located at the tails of the size distribution govern properties such as fatigue life[15,16] or shear strength,[17,18] and it is therefore critical to section large volumes of material to gain access to the microstructural statistics. For these reasons, application of existing tomographic techniques to multiphase materials, where phases with similar densities are intermixed at the μm-scale and dispersed on the mm-scale, is particularly challenging. While femtosecond lasers have been used for controlled removal of layers of atoms in conjunction with a large applied electric field in current atom-probe tomography instruments,[19] in this paper we describe a new tomographic imaging technique that addresses much larger volumes of data. Here the femtosecond laser serves as the primary material removal tool, permitting the direct ablation of material for the analysis of mm^3 volumes. This rapid serial sectioning technique utilizes high repetition rate, ultrashort femtosecond pulses for layer-by-layer material ablation that is applicable to a wide variety of materials.

Femtosecond lasers can controllably remove large volumes of material due to the high focused beam intensities ($>10^{18}$ W cm^{-2}), high laser repetition rate in the kHz range, and ultrashort femtosecond (fs) laser pulses. The tightly focused conditions (~1 μm diffraction limited spot size) obtainable with these lasers make micromachining possible without producing large heat-affected zones[20] or significant collateral dislocation damage or local melting.[21] Single pulse laser ablation studies also support femtosecond laser machining of multiphase systems with comparable material ablation rates. [22,23]

Our newly developed femtosecond laser-based technique utilizes a serial sectioning approach[2,3] involving: (1) laser ablation to remove a known amount of material from the sample surface and (2) optical imaging of the freshly ablated surface with no subsequent surface preparation required. These two steps are iterated for the desired number of slices to section a predetermined volume of material. A four-axis programmable stage provides an automated framework for translating the fixed sample between the laser beam-path to the optical microscope (see **Figure 1**). The Clark MXR CPA 2001 pulsed laser used in this sectioning experiment has the following operating conditions: 1 kHz repetition rate, 780 nm wavelength, and 150 fs pulse-width. The ablation event and incoming laser pulses are orthogonally incident to the sample surface, with a forced air stream flowing parallel to the sample surface to remove airborne ablatants. Laser machining is subsequently performed by the aggregate of millions of pulses distributed uniformly over the sample surface via the programmed stage motion pattern.

M. P. Echlin
Materials Department
University of California Santa Barbara
Building 503, Santa Barbara
CA 93106–5050 USA and Materials Science Engineering Department
University of Michigan
3062D HH. Dow Building–2300 Hayward Street Ann Arbor, MI 48109 USA
E-mail: mechlin@umich.edu
N. S. Husseini
Department of Applied Physics
2477 Randall Laboratory–450 Church St. Ann Arbor, MI 48109, USA
J. A. Nees
Center for Ultrafast Optical Science
1012 Gerstacker Bldg. 2200 Bonisteel Blvd, Ann Arbor, MI 48109, USA
Prof. T. M. Pollock
Materials Department, Building 503, Room 1355, Santa Barbara,
CA 93106–5050 USA

DOI: 10.1002/adma.201003600

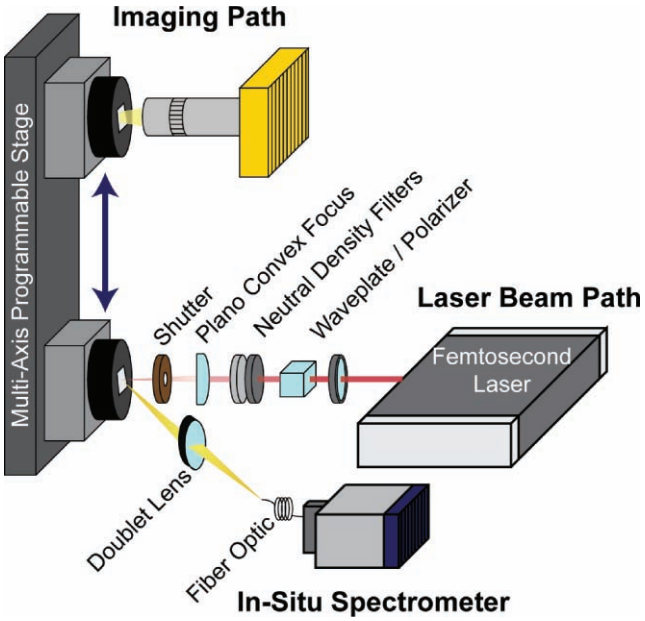

Figure 1. Schematic of the femtosecond laser aided serial sectioning technique showing a sample affixed to a 4-axis programmable stage that translates between the optical imaging path and the laser machining path with laser induced breakdown spectroscopy (LIBS) diagnostic equipment.

The machining pattern has 50% and 75% pulse overlap in the scan direction and between incremental scan lines, respectively. The sample stage is accelerated to constant velocity before the fast acting shutter opens to allow pulse deposition. By removing material uniformly layer-by-layer (see **Figure 2**a) with minimal redeposition on the sample surface, an average surface roughness of 100 nm can be achieved.

To establish relevant laser operating conditions for uniform ablation of 4330 steel containing small titanium nitride (TiN) particles, a series of single pulse studies were performed on the sample material. Peak threshold damage fluences for ablation (E_{th}) of TiN and titanium modified (Ti. mod.) 4330 steel were measured to be 0.19 and 0.41 J cm^{-2}, respectively. Atomic force microscopy (AFM) measurements on material removal rates in both TiN and the surrounding steel in this range of fluence demonstrate that the ablation depth per pulse for these two materials differs by less than 10 nm per pulse (see **Figure 3**a).[22,23] Published ablation data for a wider set of materials (see Figure 3b)[22,24–27] demonstrate that many different materials can be simultaneously and uniformly ablated in the low fluence regime, <1 J cm^{-2}, permitting acquisition of 3D information on most multiphase materials.

Images are captured optically during the sectioning experiment using a high-resolution color CCD. Once initial parameters are defined, the fully automated MATLAB processing routines segment the raw images from the femtosecond laser sectioning experiment and identify the phases or particles of interest. In the Ti. mod. 4330 steel system, the optically imaged TiN particles appear red due to absorption contrast, providing a mechanism by which image processing scripts can identify this particle type. The algorithm filters the dataset to remove periodic machining artifacts, and then uses a seed-fill algorithm to size the particles and segment them into binary images. In Figure 2b, we show a set of images generated by stacking segmented 2D images with a spacing equal to the depth of the laser slice removal rate. A 3D mesh is subsequently fit to the 3D stack using IDL (Interactive Data Language) visualization or PARAVIEW.

A set of three orthogonal 2D optical images has been assembled in (**Figure 4**a) to show schematically the size and distribution of the TiN particles. A 3D reconstructed dataset collected with the new 3D tomographic laser sectioning process is shown in (Figure 4b). This 3D dataset is composed of 407 slices with a sampling thickness of 230 nm slice^{-1} and an in-plane imaging resolution of 150 nm pixel^{-1}. The total volume of this reconstructed dataset is 315 × 156 × 89 μm. The femtosecond laser machining step of the serial sectioning process for a single 1.5 × 1.5 mm region requires approximately 7 minutes, for deposition of 2 × 10^4 pulses to remove a slice of 230 nm thickness (see Figure 2). The total acquisition time for the reconstructed 4330 steel dataset was 41 hours, with no human supervision required beyond the initial setup.

Statistical analysis of the dataset in (see Figure 2) was performed using IDL routines to calculate the volume fraction of TiN particles, 0.028%; the particle density, 2.84 × 10^{13} particle m^{-3}; the mean particle diameter, 2.12 μm; the mean nearest-neighbor distance, 10.0 μm; and total number of particles, 112. The detection limit for the image processing code is the smallest identifiable particle or 7 pixels in size (~0.1 μm^3). Additional datasets have been sampled, creating a large pool of

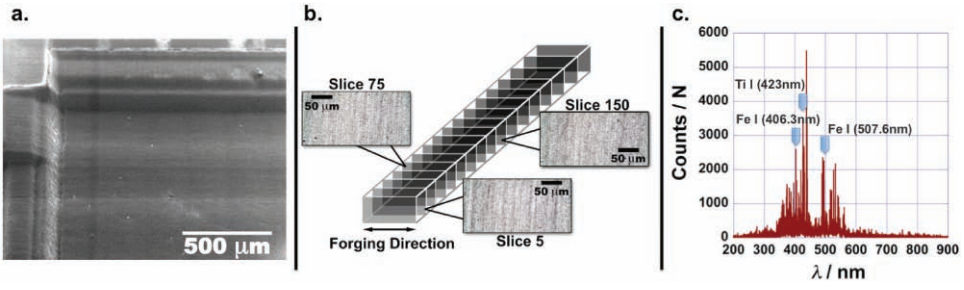

Figure 2. a) SEM image showing the laser machined area after a sectioning experiment. Laser machining induced roughness on the order of hundreds of nm and uniformly removed material is apparent from the flat contour of the lower (machined) area. b) An image stack of segmented 2D slices produced from the sectioning procedure on a Ti. mod. 4330 steel sample. The expanded images show raw color CCD optical micrographs with the red colored TiN particles. c) LIBS spectrum of Ti. mod. 4330 steel. Ti I ionization peaks are visible and can be monitored qualitatively to find TiN inclusions within each individual single pulsed area.

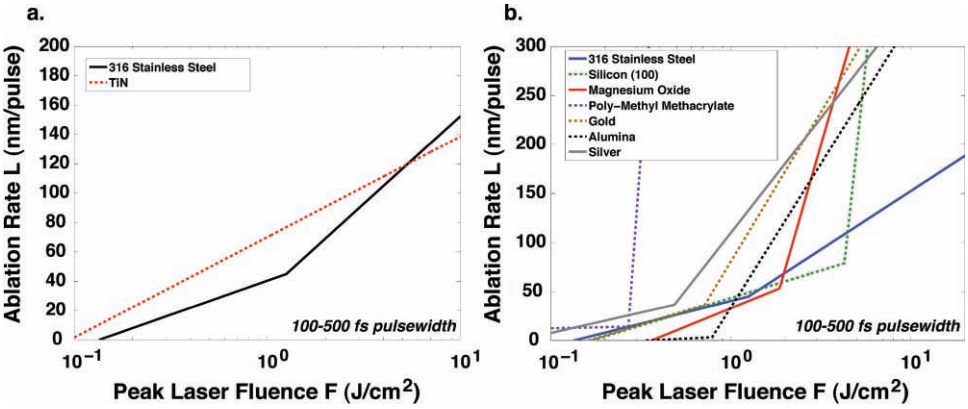

Figure 3. a) 316 stainless steel (SS)[22] and TiN[23] ablation depth per pulse data. Fluences from 3–5 J cm^{-2} produce equal removal rates in both 316 SS and TiN. Fluences between 0.1–3 J cm^{-2} can yield removal rates that are within 10 nm pulse^{-1} for the two materials. b) Various metals, ceramics, and polymer ablation rates across fluences taken from literature. [22,24–27] Multi-phase materials can be theoretically removed uniformly where these curves intersect. Ablation depths in the low fluence ablation regime tend to have values between 50–100 nm pulse^{-1}.

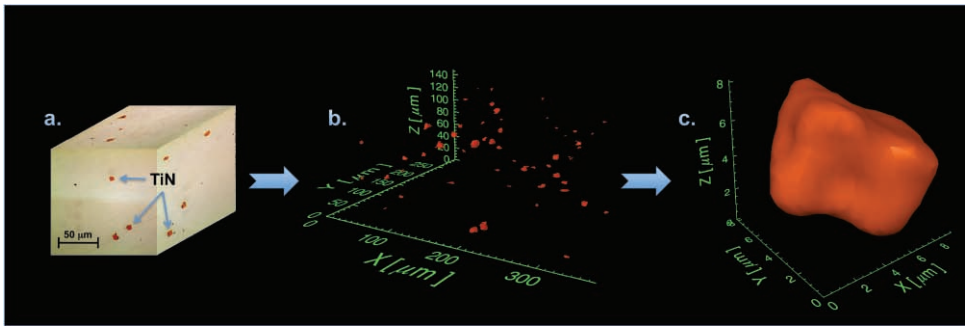

Figure 4. a) A representative orientation view of three orthogonal optical 2D images collected from the as-received Ti. mod. 4330 steel. Red TiN particles are shown in both the reconstructions (b) and the optical micrograph image (a). b) 3D reconstructions of TiN particles in the 4330 steel matrix. The imaging plane is the x-y plane, and the sectioning direction is along the z-axis. (c) Single TiN particle reconstruction with near cuboidal morphology and a size of ~6 µm.

statistical data. The datasets are captured from different locations in the bulk specimen to identify local variation in nitride densities. These statistical parameters combined with the 3D spatial distribution of the inclusion phases provide important quantitative information for input to models for failure under ballistic impact conditions,[28] specifically in the process zone, where material undergoes shear localization.

With the current optical imaging setup, this technique resolves TiN particles of diameter larger than 1 µm. Imaging resolution enhancements, including in-situ scanning electron microscopy (SEM) directly coupled with femtosecond laser machining and the integration of laser induced breakdown spectroscopy (LIBS), are currently being developed to improve resolution by an order of magnitude–approaching the resolvable limit accessible through the laser machined surface roughness. These enhancements are being integrated using a dual-beam SEM and focused ion beam system with a laser access port to ablate material in vacuum. The improved imaging resolution for femtosecond laser-based sectioning under vacuum in a SEM are reflected in **Table 1**.

LIBS spectra distinguished TiN phases from other oxide phases in the material during the machining process. With LIBS, the light generated during plasma formation is collected through a fiber optic cable, gated using a photomultiplier, separated into relative wavelengths using gratings and a prism, and projected onto a spectrographically sensitive charge-coupled device camera. This technique has identified chemical species contained in turbine blade coatings,[29] carbon content in steels,[30] minerals in biological material,[31] and elemental constituents in coral.[32] In Figure 2c, a single pulse LIBS spectrum of Ti. mod. 4330 steel contains intense first ionization

Table 1. Comparison of various sectioning techniques: atom probe tomography (APT), focused ion beam serial sectioning (FIB-SS), mechanical serial sectioning (Mech-SS), femtosecond laser serial sectioning (F/S)

	Removal rate [µm^3 s^{-1}]	Slice thickness [nm]	Resolution [nm]	Addressable volume [µm^3]
APT	10^{-8}	10^{-1}	0.5	10^{-3}–10^{-4}
FIB-SS	0.5	5–100	10–30	10^{4}–10^{5}
Mech-SS	200	100–2700	250	10^{7}–10^{10}
FSL-SS	10^{4}–10^{5}	20–150	250 (10–30)[a)]	10^{7}–10^{10}

[a)]SEM assisted FSL-SS

peaks for titanium and iron. The LIBS identification technique can be employed to collect simultaneously real-time structural and chemical information from the plasma generated in the material ablation process.

To date we have demonstrated that femtosecond laser aided serial sectioning setup is a fast, volumetrically versatile, and automated tomographic technique able to reconstruct multiphase material systems. Other multiphase materials examined during the development of this technique include the following: nickel alloys with carbide constituents, layered zirconia intermetallic NiAl systems, and fibrous Mg alloy alumina composites. Material removal rates of 10^5 μm^3 s^{-1} have been demonstrated, which is approximately 5 orders of magnitude faster than recently-developed focused ion beam tomography techniques.[3] Further improvements in material removal rates are possible with laser improvements such as higher pulse repetition rates, increased power, different focusing conditions, and improved scanning protocols. This new tomography technique will be particularly useful for imaging multiphase systems containing phases with similar densities, which are difficult to image with other fast tomographic techniques such as X-ray imaging. In Table 1, a comparison of the removal rate, slice thickness, resolution, and addressable sample volumes are given for some common serial sectioning techniques. The presented sectioning techniques span a range of addressable material and microstructural lengthscales. Major limitations of the various techniques include the speed and precision with which material can be removed. The femtosecond laser-based technique has a removal rate many orders of magnitude faster than the other techniques with a resolution that permits the analysis of sub-micron scale features. Finally, the inherent non-contact mode of laser machining also gives ample opportunity to section materials in vacuum and take advantage of other analysis techniques designed to operate in that environment, such as electron backscattered diffraction (EBSD) and energy dispersive X-ray spectroscopy (EDS).

Experimental Section

Femtosecond laser pulses were focused to e^{-2} spot radius of 36.5 μm using a 350 mm focal length plano-convex BK-7 glass lens. The sample was translated in the laser beam path using Newport mid-range linear stages with 0.5 μm resolution and 1.5 μm repeatability. A fast acting shutter regulated laser pulse deposition to occur when the stage has achieved a constant velocity state. Laser pulse energy was attenuated using a half-order waveplate rotator and polarizing cube and neutral density filters. Spectral plasma emissions for LIBS were collected using a 3 cm focal length achromatic doublet BK-7 glass lens focused onto a 50 μm fiber coupled to an Andor Mechelle 5000 spectrometer and iCCD.

Supporting Information

Supporting Information is available from the Wiley Online Library or from the author.

Acknowledgements

Support for this research came from the ONR/DARPA D3D project grant W00014–05-C-0241. The authors would also like to thank Chris Torbet for ongoing engineering support, Alessandro Mottura for useful discussions, and Dave Rowenhorst and Herng-Jeng Jou for IDL code and discussions. This article is part of the Special Issue on Materials Research at the University of California, Santa Barbara.

Received: October 1, 2010
Published online: February 25, 2011

[1] M. V. Kral, G. Spanos, *Acta Mater.* **1999**, *47*, 711.
[2] J. Alkemper, P. W. Voorhees, *J. Microsc.* **2001**, *201*, 388.
[3] M. D. Uchic, M. A. Groeber, D. M. Dimiduk, J. P. Simmons, *Scripta Mater.* **2006**, *55*, 23.
[4] J. Spowart, H. Mullens, B. Puchala, *JOM-J. Min. Met. Mat. S.* **2003**, *55*, 35.
[5] J. Madison, J. Spowart, D. Rowenhorst, T. M. Pollock, *JOM-J. Min. Met. Mat. S.* **2008**, *60*, 26.
[6] S. Hata, K. Kimura, H. Gao, S. Matsumura, M. Doi, T. Moritani, J. S. Barnard, J. R. Tong, J. H. Sharp, P. A. Midgley, *Adv. Mater.* **2008**, *20*, 1905.
[7] W. Treimer, M. Strobl, A. Hilger, C. Seifert, U. Feye-Treimer, *Appl. Phys. Lett.* **2003**, *83*, 398.
[8] A. B. Phillion, S. L. Cockcroft, P. D. Lee, *Scripta Mater.* **2006**, *55*, 489.
[9] P. G. Kotula, M. R. Keenan, J. R. Michael, *Microsc. Microanal.* **2006**, *12*, 36.
[10] A. Kumar, C. J. Torbet, J. W. Jones, T. M. Pollock, *J. Appl. Phys.* **2009**, *106*, 024904.
[11] M. N. Shabrov, A. Needleman, *Model. Simul. Mater. Sc* **2002**, *10*, 163.
[12] Y. Huang, *Mech. Mater.* **1993**, *16*, 265.
[13] E. E. Underwood, *Quantitative stereology*, Addison-Wesley, Reading, MA, USA, **1970**, 274.
[14] R. T. Dehoff, *J. Microsc.* **1983**, *131*, 259.
[15] Y. Tjiptowidjojo, C. Przybyla, M. Shenoy, D. L. McDowell, *Int. J. Fatigue* **2009**, *31*, 515.
[16] P. J. Laz, B. M. Hillberry, *Int. J. Fatigue* **1998**, *20*, 263.
[17] J. G. Cowie, M. Azrin, G. B. Olson, *Metall. Trans. A* **1989**, *20*, 143.
[18] A. S. Argon, J. Im, R. Safoglu, *Metall. Trans. A* **1975**, *6A*, 825.
[19] B. Gault, F. Vurpillot, A. Vella, M. Gilbert, A. Menand, D. Blavette, B. Deconihout, *Rev. Sci. Instrum.* **2006**, *77*, 043705.
[20] P. P. Pronko, S. K. Dutta, J. Squier, J. V. Rudd, D. Du, G. Mourou, *Opt. Commun.* **1995**, *114*, 106.
[21] Q. Feng, Y. N. Picard, H. Liu, S. M. Yalisove, G. Mourou, T. M. Pollock, *Scripta Mater.* **2005**, *53*, 511.
[22] P. T. Mannion, J. Magee, E. Coyne, G. M. O'Connor, T. J. Glynn, *Appl. Surf. Sci.* **2004**, *233*, 275.
[23] N. Yasumaru, K. Miyazaki, J. Kiuchi, *Appl. Phys. A: Mater. Sci. Process.* **2005**, *81*, 933.
[24] E. Coyne, J. P. Magee, P. Mannion, G. M. O'Connor, T. J. Glynn, *Appl. Phys. A: Mater. Sci. Process.* **2005**, *81*, 371.
[25] J. Ihlemann, A. Scholl, H. Schmidt, B. Wolff-Rottke, *Appl. Phys. A: Mater. Sci. Process.* **1995**, *60*, 411.
[26] M. Obara, H. Yabe, Y. Hirayama, K. Takahashi, K. Furusawa, F. Barnier, Y. P. Kim, in *High-Power Laser Ablation III*, (Ed: C. R. Phipps), SPIE, Santa Fe, NM, USA, **2000**.
[27] A. A. Serafetinides, M. I. Makropoulou, C. D. Skordoulis, A. K. Kar, *Appl. Surf. Sci.* **2001**, *180*, 42.
[28] F. Vernerey, W. Liu, B. Moran, G. B. Olson, *Comput. Mech.* **2009**, *44*, 433.
[29] J. P. McDonald, D. K. Das, J. A. Nees, T. M. Pollock, S. M. Yalisove, *Spectrochim. Acta B* **2008**, *63*, 561.
[30] J. A. Aguilera, C. Aragon, J. Campos, *Appl. Spectrosc.* **1992**, *46*, 1382.
[31] M. Corsi, G. Cristoforetti, M. Hidalgo, S. Legnaioli, V. Palleschi, A. Salvetti, E. Tognoni, C. Vallebona, *Appl. Opt.* **2003**, *42*, 6133.
[32] S. Pandhija, A. Rai, *Appl. Phys. B: Lasers Opt.* **2009**, *94*, 545.